BIOPSY NEEDLE TRACT CAUTERIZATION USING AN EMBEDDED ARRAY OF PIEZOCERAMIC MICROHEATERS

Karthik Visvanathan and Yogesh B. Gianchandani
University of Michigan, Ann Arbor, USA

ABSTRACT

This paper presents the use of an array of piezoceramic microheaters embedded in a biopsy needle for tract cauterization. Circular PZT-5A heaters of 200 µm diameter and 70-80 µm thickness are embedded in the wall of a 20-gauge stainless steel needle. Finite element modeling suggests that a PZT array with no gap between the elements to be the most suitable design. The temperature profile generated is measured at two resonance modes: the radial mode (10.3 MHz) and the thickness mode (22.3 MHz). The needle surface exceeds the minimum target temperature rise of 33˚C for applied voltages of 17 V_{RMS} and 14 V_{RMS} for radial and thickness mode, respectively. The corresponding input powers are 236 mW and 325 mW, respectively. The tissue cauterization extends 1-1.25 mm beyond the perimeter of needle.

INTRODUCTION

Needle aspiration biopsy is a diagnostic procedure used to investigate thyroid, breast, liver and lung cancers [1]. Even though percutaneous biopsies are generally safe, there have been reports of potential risks such as deposition of viable tumor cells or "seeding" along the needle tract. The rate of seeding can vary from 5.1%-12.5% [2]. Studies also suggest that post biopsy hemorrhage (bleeding) can be as high as 18.3%-23% [3]. Further, this percentage can be higher for patients with cirrhosis and uncorrected coagulopathy [4]. The development of an effective, inexpensive and simple method of cauterization of needle tracts could minimize the risk of bleeding and needle tract seeding (Fig. 1).

Past work had been limited to using radiofrequency (RF) ablation of needle tracts. Animal studies of RF coagulation with use of the biopsy needle itself were discussed in [5]. In this method, the outside of the biopsy needle, except for the last two centimeters, was coated with a thin layer of electrical insulation. A source of RF electrical power was then connected to the biopsy needle as it was withdrawn from the body, to provide electro cauterization of the needle tract. Comparison of hemorrhage after liver and kidney biopsy, with and without ablation of the needle tract, was reported in [4]. Here, RF ablation by an introducer needle was employed as the ablation procedure. This study suggested that RF ablation reduces bleeding as compared to absence of RF ablation, in liver and kidney procedures, with mean blood loss reduced by 63% and 97%, respectively.

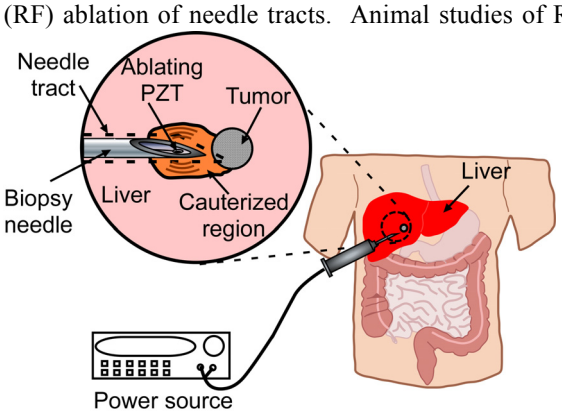

Figure 1: Concept diagram of a biopsy tool with cauterization capability.

Other cauterization methods have not been explored, possibly due to the difficulty of integration with the biopsy needles. In particular, ultrasonic heating using piezoceramics holds significant promise as it can possibly be combined with ultrasonic tissue density measurements [6] for determining completion of tissue cauterization. Heat generation in 3.2 mm diameter lead zirconate titanate (PZT) discs for biological tissue cauterization has been reported in [7]. We now describe experiments using array of 200 µm diameter bulk micromachined PZT transducers with a 20-gauge biopsy needle for cauterization of the needle tract. The following sections present the simulation model, device design and fabrication, and experimental results for porcine tissue cauterization using the proposed biopsy tool.

SIMULATION MODEL

A 3D finite element model has been developed to estimate the temperature profile in the tissues. Pennes' bioheat transfer model [8] is used to model heat transfer in tissues. This model takes into account the cooling due to blood flow in tissues. The model is given by:

$$\rho_t c_t \frac{\partial T}{\partial t} = \nabla . k \nabla T + \rho_b c_b \omega_b \left(T_b - T\right) + \dot{q} \quad (1)$$

where ρ_t is the density of the medium, c_t is the specific heat capacity, k is the thermal conductivity, T is the temperature, ρ_b is the density of blood, c_b is the specific heat capacity of blood, ω_b is the perfusion rate of the blood, T_b is the arterial blood temperature and q is the heat generation rate per unit volume due to ultrasound applicator.

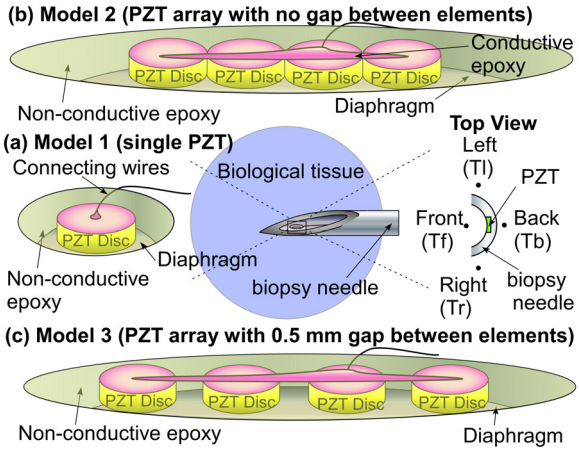

Figure 2: Schematic model of various biopsy tool designs considered in the simulation.

For the structure used in this work, PZT heaters are significantly smaller than the size of the needle. Hence the heaters are modeled as small spherical sources. The heat generation rate from the PZT heater is given by [9]:

$$\dot{q} = \frac{2\alpha I_s r_0^2}{r^2} e^{-2\mu(r - r_0)} \qquad (2)$$

where α is the ultrasound absorption coefficient ($Np.m^{-1}$), I_s is the ultrasound intensity along the surface of the transducer (Wm^{-2}), r is the radial distance from the center of the transducer and r_0 is the radius of the transducer. The term μ is the ultrasound attenuation and is taken equal to α under the assumption that all the attenuated acoustic energy is absorbed by the local medium. However, due to inefficiencies in the transducer, not all the electrical energy applied to it gets converted into acoustic energy. This unconverted energy is dissipated as heat within the transducer. For a given transducer efficiency, ν, the heat generation rate per unit volume within the transducer is given by:

$$\dot{q}_{app} = \left(\frac{1-\nu}{\nu}\right)\frac{3I_s}{r_0} \qquad (3)$$

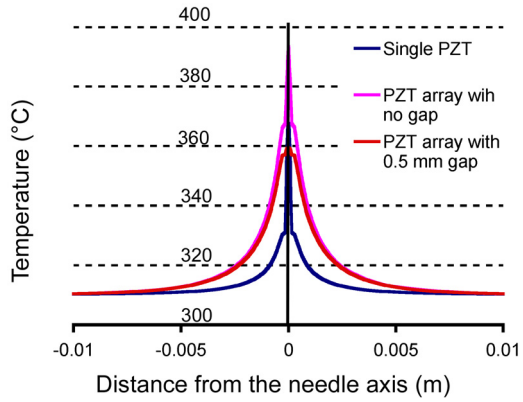

Figure 3: Finite element simulation results for the variation of temperature as a function of distance from the needle for the three designs for an ultrasound intensity, I_s = 90 Wcm^{-2}.

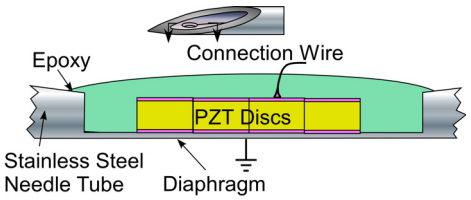

Figure 4: Schematic diagram of the proposed biopsy tool.

The simulations were performed using the bioheat equation model in COMSOL Multiphysics 3.4. Three designs were considered in the simulations: single PZT disc, PZT array (4 discs) with no gap between elements, and PZT array with 0.5 mm gap between elements (Fig. 2). All these models consisted of four major regions: PZT heater, epoxy surrounding the PZT heater, biopsy needle and biological tissue. The biological tissue was modeled using a 5 cm diameter sphere surrounding the needle. The 20 gauge needle used in the experiments was modeled using a partial cylinder with inner and outer radii of 300 µm and 450 µm, respectively. The length of the needle was 6 cm. For a single PZT design, a hole of 135 µm depth and 300 µm diameter was created to model the cavity for placing the PZT heater. In the case of array design, a slot of 2000x300x135 μm^3 was created in the needle. The material properties used in the simulations are shown in Table 1.

The cooling due to blood flow was considered only in the biological tissue region. The heat generation rate given in equation 2 was used in epoxy, needle and tissue region. The heat generation rate given by equation 3 was used in the PZT region. The outer surface of the tissue and the far end tip of the needle (outside the tissue region) were maintained at 310 K and 300 K, respectively. In the simulations, transducer efficiency was assumed to be 0.52. Figure 3 compares the simulation results for temperature variation as a function of distance from the needle. Simulations suggest that for an ultrasonic surface

Table 1:Material properties used in the simulations

Density of tissue	1050 kgm^{-3}
Thermal conductivity of tissue	0.51 $Wm^{-1}K^{-1}$
Specific heat capacity of tissue	3639 $Jkg^{-1}K^{-1}$
Density of blood	1000 kgm^{-3}
Specific heat capacity of blood	4180 $Jkg^{-1}K^{-1}$
Perfusion rate of blood	15x10^{-3} s^{-1}
Arterial blood temperature	310 K
Thermal conductivity of needle	44.5 $Wm^{-1}K^{-1}$
Density of needle	7850 kgm^{-3}
Specific heat capacity of needle	475 $Jkg^{-1}K^{-1}$
Thermal conductivity of epoxy	1.7 $Wm^{-1}K^{-1}$
Density of epoxy	1060 kgm^{-3}
Specific heat capacity of epoxy	1000 $Jkg^{-1}K^{-1}$
Thermal conductivity of PZT	1 $Wm^{-1}K^{-1}$
Density of PZT	7700 kgm^{-3}
Specific heat capacity of PZT	350 $Jkg^{-1}K^{-1}$

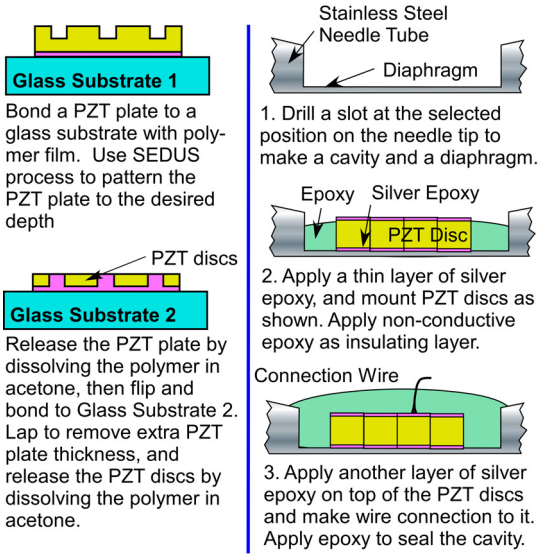

Figure 5: (a) Ultrasonic machining process for PZT disc fabrication [10]. (b) PZT disc integration procedure for the biopsy tool.

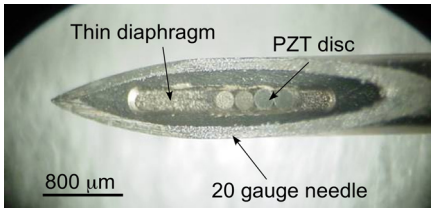

Figure 6: Photograph of the biopsy needle with four PZT discs integrated into a slot in a 20 gauge needle.

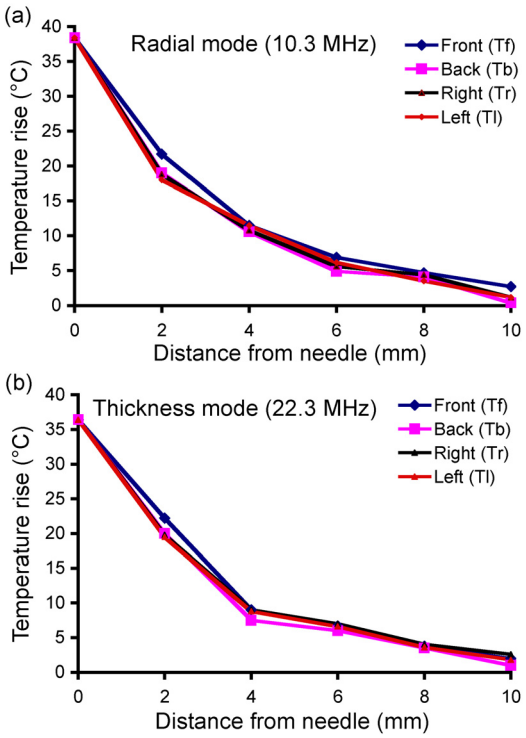

Figure 7: Variation of temperature as a function of direction (Fig. 2) and distance from the needle for (a) radial mode and (b) thickness mode resonances.

intensity (that is proportional to drive voltage) of 90 Wcm^{-2}, maximum temperature is attained by PZT array with no gap between the elements.

DEVICE DESIGN AND FABRICATION

The schematic of the proposed biopsy tool design is shown in Fig. 4. The PZT discs were fabricated from PZT-5A material. This material has a Curie temperature of 350˚C, which is greater than the target temperature of 70-100˚C (ΔT=33-63˚C). Circular shaped PZT devices were used because for a given volume device, these generate higher temperature rise per unit voltage as compared to square and rectangular devices [7].

The PZT discs (diameter =200 µm; thickness =70-80 µm) were fabricated using an ultrasonic micro-machining process (USM) [10] (Fig. 5a). The USM tools were fabricated using micro electro-discharge machining (µ-EDM) of stainless steel. The pattern was then transferred to the PZT-5A plate using USM with tungsten carbide slurry. The patterned PZT discs were released by lapping from behind. Finally, a 500 nm thick gold layer was sputtered to form the electrodes. The sides of the discs were covered with a thin layer of photoresist to prevent shorting of the two electrodes during sputtering. The PZT discs were integrated into a recess (2000x300x135 μm^3) cut into a 20-gauge needle using µ-EDM (Fig. 5b, 6). This prevents the discs from blocking the path for acquiring tissues during the biopsy process. The thin diaphragm left behind in the wall of the needle after the formation of recess, also reduces the heat loss due to conduction through the needle. The PZT discs were surrounded by non-conductive epoxy in order to provide a highly damping medium for heat generation as well as reduce heat loss due to conduction. Flexible copper wire within lumen provided power to the top electrode while the needle provided the ground return path.

EXPERIMENTAL RESULTS

The temperature profile generated by the biopsy tool was measured at two resonance modes: the radial mode (10.3 MHz) and the thickness mode (22.3 MHz). PZT discs were actuated using a sinusoidal wave at the respective resonance frequencies using a function generator amplified using a power amplifier. The temperature was measured using a K-type thermocouple read using a digital thermometer. The experiments were performed by inserting the needle into porcine tissue samples. Figures 7a and 7b show the temperature measured at different distances and directions from a needle for the radial and thickness mode resonances, respectively. The temperature distribution is similar in all directions for both resonance modes. This indicates uniform cauterization in the surrounding region.

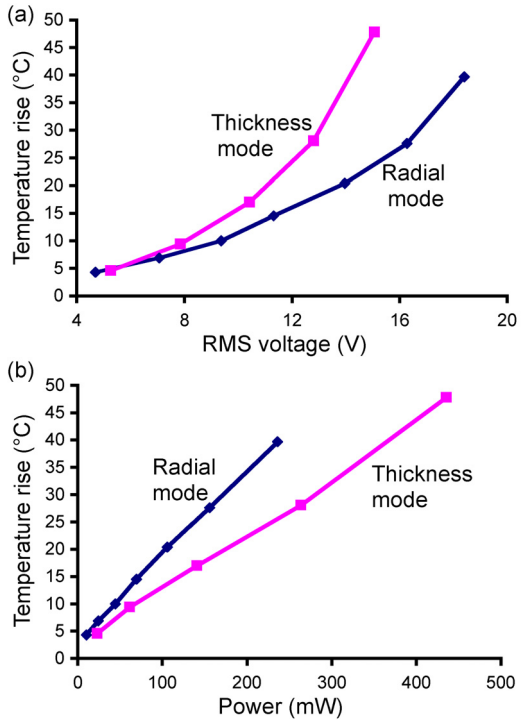

Figure 8: Variation in the temperature generated at the surface of the needle for various (a) input voltages and (b) input power.

The temperature rise at the surface of needle, in both resonance modes, for varying input voltage is shown in Fig. 8a. The needle surface exceeded the minimum target temperature rise of 33˚C for an applied voltage of 17 V_{RMS} and 14 V_{RMS} for radial and thickness mode, respectively. Figure 8b compares the temperature rise generated at the surface of the needle for various input power for the two modes. The plot suggests that the target temperature rise of 33˚C was achieved for input power of 236 mW and 325 mW, respectively. This difference is believed to be mainly due to the higher electromechanical impedance of the PZT device at lower operating frequency. Figure 9 shows the photographs of the cauterized porcine tissue for an applied voltage of 14V_{RMS} at 22.3 MHz. The radius of tissue cauterization is 1-1.25 mm beyond the perimeter of needle. This ensures minimal damage to the surrounding healthy tissue.

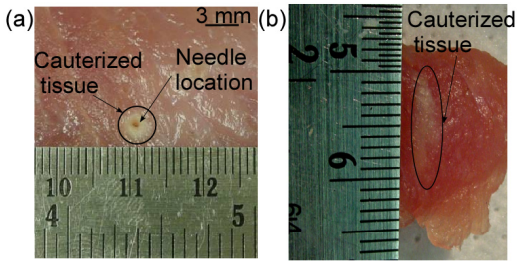

Figure 9: Photograph of (a) top view and (b) cross section of the cauterized porcine tissue. The radius of cauterization beyond perimeter of needle was 1-1.25 mm for an input RMS voltage of 14 V.

CONCLUSIONS

The use of embedded piezoceramic heaters for biopsy needle tract cauterization to prevent tumor seeding and post biopsy hemorrhage is discussed. A finite element model is used to predict the temperature profile generated by these heaters. The PZT heaters generate the target temperature rise of 33˚C for an input power of <325 mW and drive voltage of <17 V_{RMS}. The extent of tissue cauterization was <1.25 mm beyond the perimeter of the needle thereby ensuring minimum damage to the surrounding tissues. This approach bears significant promise in the long term to combine cauterization with ultrasonic tissue density measurements as described in [6].

ACKNOWLEDGEMENTS

The authors would like to thank Dr. Tao Li for his guidance in biopsy needles and ultrasonic machining. This work was supported in part by a fellowship to KV from the UM Department of Mechanical Engineering.

REFERENCES

[1] R.G. Amedee et al., "Fine needle aspiration biopsy," *The Laryngoscope,* 111, pp.1551-1557, 2001

[2] A. Pelloni, et al., "Risks and consequences of tumor seeding after percutaneous fine needle biopsy for diagnosis of hepatocellular carcinoma," *Schweiz Med Wochenschr,* 130, pp. 871–877, 2000

[3] S. Sugano, et al., "Incidence of ultrasound-detected intrahepatic hematomas due to Tru-cut needle liver biopsy," *Digestive diseases and Sciences,* 36, pp. 1229–1233, 1991.

[4] W.F. Pritchard et al., "Radiofrequency cauterization with biopsy introducer needle," *J Vasc Interv Radiol,* 15, pp. 183-187, 2004.

[5] E.H. Kim et al., "Electrocautery of the tract after needle biopsy of the liver to reduce blood loss: Experience in the canine model," *Investigative Radiology*, 28, pp. 228 –230, 1993.

[6] T. Li et al., "Micromachined bulk PZT tissue contrast sensor for fine needle aspiration biopsy**,"** *Lab Chip*, 7, pp. 179-185, 2007.

[7] K. Visvanathan et al., "Ultrasonic microheaters using piezo-ceramics for cauterization and other applications," *IEEE Transducers,* pp. 2421–24, 2009.

[8] H.H. Pennes, "Analysis of tissue and arterial blood temperature in the resting human forearm," *J. App. Physiol.,* 1, pp. 93-122, 1948.

[9] M.G. Skinner et al., "A theoretical comparison of energy sources- microwave, ultrasound and laser- for interstitial thermal therapy," *Phys. Med. Biol.,* 43, pp. 3535-3547, 1998

[10] T. Li et al., "A micromachining process for die-scale pattern transfer in ceramics and its application to bulk piezoelectric actuators," *JMEMS,* 15, pp. 605-612, 2006.